Original Article

DOI: 10.5582/bst.2017.01311

Shenqi detoxification granule combined with P311 inhibits epithelial-mesenchymal transition in renal fibrosis *via* TGF-β1-Smad-ILK pathway

Pingping Cai[1], Xiang Liu[2], Yuan Xu[1], Fanghua Qi[1], Guomin Si[1,*]

[1] *Department of Traditional Chinese Medicine, Shandong Provincial Hospital affiliated to Shandong University, Ji'nan, China;*
[2] *Department of Nephrology, Shandong Provincial Hospital affiliated to Shandong University, Ji'nan, China.*

Summary **Shenqi detoxification granule (SDG), a traditional Chinese herbal formula, has been shown to have nephroprotective and anti-fibrotic activities in patients with chronic kidney disease (CKD). However, its mechanisms in renal fibrosis and the progression of CKD remain largely unknown. P311, a highly conserved 8-kDa intracellular protein, plays a key role in renal fibrosis by regulating epithelial-mesenchymal transition (EMT). Previously, we found P311 might be involved in the pathogenesis of renal fibrosis by inhibiting EMT *via* the TGF-β1-Smad-ILK pathway. We also found SDG combined with P311 could ameliorate renal fibrosis by regulating the expression of EMT markers. Here we further examined the effect and mechanism of SDG combined with P311 on TGF-β1-mediated EMT in a rat model of unilateral ureteral occlusion (UUO) renal fibrosis. After establishment of the UUO model successfully, the rats were gavaged with SDG daily and/or injected with recombinant adenovirus p311 (also called Ad-P311) through the tail vein each week for 4 weeks. Serum creatinine (Cr), blood urea nitrogen (BUN) and albumin (ALB) levels were tested to observe renal function, and hematoxylin eosin (HE) and Masson staining were performed to observe kidney histopathology. Furthermore, the expression of EMT markers (E-cadherin and α-smooth muscle actin (α-SMA)) and EMT-related molecules TGF-β1, pSmad2/3, Smad7 and ILK were observed using immunohistochemical staining and Western blot analysis. Treatment with SDG and P311 improved renal function and histopathological abnormalities, as well as reversing the changes of EMT markers and EMT-related molecules, which indicated SDG combined with P311 could attenuate renal fibrosis in UUO rats, and the underlying mechanism might involve TGF-β1-mediated EMT and the TGF-β1-Smad-ILK signaling pathway. Therefore, SDG might be a novel alternative therapy for treating renal fibrosis and delaying the progression of CKD. Furthermore, SDG combined with P311 might have a synergistic effect on attenuating renal fibrosis.**

Keywords: Shenqi detoxification granule (SDG), P311, renal fibrosis, epithelial-mesenchymal transition (EMT), TGF-β1-Smad-ILK pathway

1. Introduction

Chronic kidney disease (CKD) is an important public health problem and causes significant morbidity and mortality worldwide (*1*). Renal fibrosis is generally recognized as the most prominent feature and the common final manifestation of progressive CKD (*2*). To delay the progression of CKD, inhibition of renal fibrosis may be a key factor for developing new clinical treatment options. However, there are still few clinical treatment options, which can block the progression of CKD. Thus, many patients begin to seek out alternative therapies such as traditional Chinese medicine. Chinese herbal medicine has been used for thousands of years and has successfully treated a number of human diseases,

**Address correspondence to:*
Dr. Guomin Si, Department of Traditional Chinese Medicine, Shandong Provincial Hospital affiliated to Shandong University, No. 324, Jingwuweiqi Road, Ji'nan 250021, Shandong, China.
E-mail: sgm977@126.com

including some kidney diseases. Recently, several traditional Chinese medications with anti-inflammation, anti-oxidative, or immunomodulatory properties have attracted considerable interest as candidates for the development of novel CKD therapeutics (*3*).

Shenqi detoxification granule (SDG), a traditional Chinese herbal formula, has been used in the clinic for the treatment of CKD for many years (*4*). As shown in Table 1, SDG contains 12 herbs including Radix Astragali, Salvia miltiorrhiza, Angelica sinensis, and so on. According to the theoretical basis of traditional Chinese medicine, SDG possesses a function of tonifying the kidney, invigorating blood circulation and detoxifcation. In our previous basic and clinical studies, we found that SDG could decrease the levels of blood urea nitrogen (BUN), serum creatinine (Scr), and leptin, and increase the levels of albumin (ALB) (*5,6*). These findings indicated that SDG could effectively alleviate kidney injury and prevent the progress of CKD. Furthermore, the possible mechanism of SDG on inhibiting renal fibrosis might be involved in the transforming growth factor-β1 (TGF-β1)-Smad pathway in rats (*7*). However, the mechanisms of SDG in renal fibrosis and the progression of CKD remain largely unknown.

Renal fibrosis is characterized by the trans-differentiation of myofibroblasts and deposition of extracellular matrix (ECM) (*8*). During fibrosis, kidney resident cells such as fibroblasts, epithelial, endothelial or mesangial cells trans-differentiate into myofibroblasts that express and deposit excessive ECM proteins in the renal interstitial spaces, eventually leading to renal fibrosis and functional loss (*9*). Renal tubular epithelial-mesenchymal transition (EMT) is a critical step and key mechanism in the development of this condition, and about 30% of myofibroblasts are generated *via* EMT during kidney fibrosis (*10*). During the EMT process, tubular epithelial cells lose their adhesion molecules such as E-cadherin, and gain mesenchymal cell markers, such as alpha-smooth muscle actin (α-SMA), vimentin, fibronectin, and collagen I (*11*). TGF-β1 is a well-known pro-fibrotic cytokine that plays an important role in renal fibrosis (*12*). It is a major inducer of EMT that has been shown to initiate and complete the whole EMT process (*13*). Emerging data indicate that TGF-β1 induces EMT in renal fibrosis primarily *via* the Smad signaling pathway (*14*). Upon TGF-β1 binding to its receptors, Serine/Threonine kinases are activated and induce phosphorylation of Smad2/Smad3, and then phosphorylated Smad2/3 partner with Smad4 and are translocated into the nucleus where they regulate the transcription of the target genes responsible for EMT. Integrin linked kinase (ILK) is an intracellular serine/threonine kinase involved in cell-matrix interactions (*15,16*). It is shown to be a key intracellular mediator that regulates TGF-β1-induced-EMT through the Smad signaling pathway in renal tubular epithelial cells. Since EMT is the key factor by which renal fibrosis develops, inhibiting the EMT program through the TGF-β1-Smad-ILK pathway is considered a potential mechanism for anti-fibrotic therapies.

P311, an 8-kD, 68-amino acid, intracellular polypeptide, is highly conserved across species and abundantly expressed in brain, smooth muscle, regeneration tissues, and malignant glioblastomas (*17*). It can bind to TGF-β latency associated protein and stimulate the translation of TGF-β. In addition, P311 has proved to be of importance in the process of myofibroblast differentiation and fibrosis with functions of promoting embryonic development, wound healing, as well as nerve and lung regeneration, and so on (*18-22*). In our previous studies, we found that P311 might be involved in the pathogenesis of renal fibrosis by inhibiting the EMT process *via* the TGF-β1-Smad-ILK pathway *in vitro* (*23*). P311 might be a novel target for control of renal fibrosis and the progression of CKD. We also found that SDG combined with P311 could ameliorate renal fibrosis and block the progression of CKD by regulating the expression of EMT-related protein α-SMA (*24*).

In the current study, we further examined the effect of SDG combined with P311 on TGF-β1-mediated EMT in a rat model of unilateral ureteral occlusion (UUO) renal

Table 1. Formulation of Shenqi detoxification granule (SDG)

Common name	Botanical name	Voucher specimen number	Part used	Weight (g)
Radix astragali	*Astragalus membranaceus* (Fisch.) Bge	10142	Root	60
Salvia miltiorrhiza	*Salvia miltiorrhiza* Bge.	10140	Rhizome	20
Angelica sinensis	*Angelica sinensis* (Oliv.) Diels	10136	Root	12
Rheum officinale	*Rheum officinale* Baill.	10137	Root and rhizome	10
Gordon euryale seed	*Euryale ferox* Salisb.	10156	Seed	15
Herba ecliptae	*Eclipta prostrata* L.	10152	Whole plant	15
Radix semiaquilegiae	*Semiaquilegia adoxoides* (DC.) Makino	10168	Root	15
Rhizoma imperatae	*Imperata cylindrica Beauv.* var. *major* (Nees) C. E. Hubb.	10126	Root	15
Processed radix aconiti lateralis	*Aconitum carmichaelii* Debx.	10172	Root	10
Herba epimedii	*Epimedium brevicornu* Maxim.	10176	Leaf	15
Cherokee rose fruit	*Rosa laevigata* Michx.	10146	Fruit	15
Hedyotis diffusa	*Hedyotis diffusa* Willd.	10124	Whole plant	15

fibrosis. After constructing a recombinant adenovirus p311 (also called Ad-P311) and transferring it into UUO rats, the preventing effect and possible mechanisms of SDG combined with P311 on TGF-β1-mediated EMT were explored.

2. Materials and Methods

2.1. *SDG preparation*

As shown in Table 1, SDG contained twelve ingredients including Radix Astragali, Salvia miltiorrhiza, Angelica sinensis, and so on. These ingredients were ordered from Shandong Hong-Ji-Tang pharmaceutical group corporation (Ji'nan, Shandong, China), and identified by Professor Bo Xu (Department of Pharmacy, Shandong Provincial Hospital affiliated to Shandong University, Ji'nan, Shandong, China). The voucher specimen numbers of these herbs are listed in Table 1, however, they have not been deposited into a publicly available herbarium. SDG was produced according to the method reported in our previous study (*4*). Briefly, these twelve ingredients were mixed in proportion, boiled with distilled water twice, and the resulting decoction was mixed and filtered using filter paper. Then, the filtered solution was collected and concentrated to a relative density. Finally, clear paste and excipient were mixed to make sugar-free granules, then dried, granulated, packed (10 g/bag), and labeled, which contained 20 g granules of 217 g crude drugs. Then the granules were made into 0.4 mg/mL liquid and kept at 4°C.

2.2. *Animals*

Sixty male Sprague-Dawley rats (8 weeks old, 200 ± 10 g) were bought from Shandong Experimental Animal Center (Ji'nan, Shandong, China), and were given free access to water and food throughout the experiments. All animals were housed in plastic cages with a room temperature of 22 ± 1°C and relative humidity of 50 ± 10% under a 12-h light/dark cycle. The rats were acclimatized for at least 1 week prior to the experiments. All animal experimental protocols were handled in accordance with the Code of Ethics of the World Medical Association. All experimental procedures were approved by the Institutional Animal Care and Use Committee of Shandong Provincial Hospital Affiliated to Shandong University (No. 2017-208).

2.3. *Establishment of UUO model*

UUO model was performed as described previously (*25*). Briefly, after induction of general anesthesia by intraperitoneal injection of 3% pentobarbital (Sigma, St. Louis, MO, USA) (1 mL/kg body wt), the abdominal cavity was exposed *via* midline incision and the left ureter was ligated at 2 points with 4.0 silk (Niccho Kogyo Co., Ltd., Tokyo, Japan). Sham-operated rats had their ureters manipulated but not ligated and were used as controls.

2.4. *Experimental protocol*

The rats were randomly divided into six groups and given different treatments, each consisting of ten animals as follows: control group (or sham surgery group), UUO group, control + Ad-P311 group, UUO + Ad-P311 group, UUO + SDG group, and UUO + SDG + Ad-P311 group. Ad-P311 was constructed as described previously by the current authors and stored at -80°C for use (*23*). After establishment of the UUO model successfully, rats in the control group and UUO group were gavaged with 2 mL normal saline daily for 4 weeks and injected with 0.5 mL normal saline through tail vein each week for 4 weeks, while the rats in control + Ad-P311 group and UUO + Ad-P311 group were gavaged with 2 mL normal saline daily for 4 weeks and injected with 0.5 mL P311 adenovirus by tail vein each week for 4 weeks. In addition, the rats in UUO + SDG group were gavaged with 2 mL SDG daily for 4 weeks and injected with 0.5 mL normal saline through tail vein each week for 4 weeks, while the rats in UUO + SDG + Ad-P311 group were gavaged with 2 mL SDG daily for 4 weeks and injected with 0.5 mL P311 adenovirus by tail vein each week for 4 weeks.

After 4 weeks treatment, these rats were euthanized under ether and their blood and kidneys were harvested. To make the rats enter quickly into the state of anesthesia and reduce their pain and fear, inhaling ether was used as euthanasia method and this method was approved by the Institutional Animal Care and Use Committee of Shandong Provincial Hospital Affiliated to Shandong University. Serum Cr, BUN and ALB (BioVision, Inc., Milpitas, CA, USA) levels in the blood were tested using detection kits. Part of the kidney was fixed in 10% formalin solution and embedded in paraffin as 3 μm sections for hematoxylin and eosin (HE), Masson's trichrome and immunohistochemical staining. The other part of the kidney was stored at -80°C for Western blot analysis, which was performed as previously described to detect protein expression of E-cadherin, α-SMA, TGF-β1, phosphorylated Smad2/3 (pSmad2/3), Smad7 and ILK (Santa Cruz Biotechnology, Santa Cruz, CA, USA).

2.5. *Hematoxylin eosin (HE) staining and Masson staining*

To observe histological morphology changes of kidney tissue, HE staining and Masson staining were performed. First, kidney tissues were fixed with 10% neutral formaldehyde and dehydrated in graded ethanol. After permeation with xylene, they were embedded in paraffin.

Paraffin blocks were cut into 2 μm slices, mounted onto glass slides and stained using standard techniques of HE staining and Masson staining according to previous studies (*26*). Renal tubular injury index including inflammatory, cell infiltration, interstitial fibrosis, interstitial edema, cell vacuolar degeneration, tubular atrophy, and tubular expansion was measured to assess renal interstitial lesions. Ten different fields were selected to estimate the level of renal injury index with HE staining using a bio-image analysis system (Bio-Profile). Each parameter was evaluated and given a score from 0 to 4+, (0, no changes; 1+, changes affecting 5-25%; 2+, changes affecting 25-50%; 3+, changes affecting 50-75%; 4+, changes affecting 75-100%) (*28*). The severity of interstitial fibrosis was estimated by scanning 10 non-repeated fields in each sample with Masson staining. Blue-stained fibrotic areas were quantified by Image-Pro plus 6.0 software (Media Cybernetics, Rockville, MD, USA) (*27*). The results were expressed as the proportion of relative volume of scanned interstitium. All cases of HE and Masson staining were evaluated independently by two investigators and any discrepancy was resolved with a group discussion.

2.6. *Immunohistochemical staining*

To analyze the protein expression of α-SMA, pSmad2/3, and Smad7, immunohistochemistry staining assays were performed as described previously (*26*). First, paraffin sections were de-paraffinized, hydrated, and immersed in 0.3% hydrogen peroxide in methanol for 30 min to block the endogenous peroxidase activity. Second, the sections were incubated in primary antibodies (α-SMA, Smad2/3, and Smad7) overnight at 4°C, followed by incubation in anti-mouse secondary antibody for 1 h at room temperature. Third, visualization was carried out using a DAB horseradish peroxidase color development kit (Beyotime Institute of Biotechnology, Shanghai, China), and slides were counter stained in hematoxylin-1. Finally, ten random fields were examined per slice for expression of α-SMA, Smad2/3, and Smad7 using a Leica DM2500 optical microscope at a magnification of ×200. The mean optical density (MOD) was measured by Image-Pro Plus 6.0 image analysis software. All cases of immunohistochemical staining were evaluated independently by two investigators and any discrepancy was resolved with a group discussion.

2.7. *Western blot analysis*

Thirty micrograms of total cellular proteins were resolved by sodium dodecyl sulfate polyacrylamide gel electrophoresis (SDS PAGE) and transferred onto polyvinylidene fluoride (PVDF) transfer membranes for Western blot analysis (*28*). The results were quantified using Image J (National Institutes of Health, Bethesda, MD, USA). The following antibodies were used: E-cadherin, α-SMA, TGF-β1, pSmad2/3, Smad7 and ILK (Santa Cruz Biotechnology, Santa Cruz, CA, USA).

2.8. *Statistical analysis*

Statistical analysis was performed using SPSS software, version 17.0 (SPSS Inc., USA). All experiments were performed in triplicate and the data were expressed as the mean ± standard deviation (SD). The statistical significance of differences were calculated using the *t*-test and one-way analysis of variance (ANOVA), and $p < 0.05$ was considered statistically significant.

3. Results

3.1. *General condition of rats*

After treatment for 4 weeks, rats in the control group and control + Ad-P311 group were still in good shape, glossy coat color and obesity, while rats in the UUO group, and SDG or Ad-P311 treatment groups had different degrees of anorexia, low spirits, matte coat color, and kidney enlargement, and even individual rats were dead from kidney failure. There were 8 deaths including 3 in the UUO group, 2 in UUO + SDG group, 2 in UUO + Ad-P311 group, and 1 in UUO + SDG + Ad-P311 group. In addition, there was a great change in body weight of rats after establishment of the UUO model and treatment with SDG or Ad-P311. As shown in Table 2, after 4 weeks of treatment, compared to control group, body weight in the UUO group ($p < 0.01$), UUO + SDG group ($p < 0.05$), UUO + Ad-P311 group ($p < 0.05$), and UUO + SDG + Ad-P311 ($p < 0.05$) group had different degrees of weight loss, while there was no significant difference in control group and control + Ad-P311 group ($p > 0.05$). Moreover, weight loss was reversed significantly by administration of SDG and Ad-P311 especially in the UUO + SDG + Ad-P311 group ($p < 0.01$) compared to that in UUO group.

3.2. *Serum levels of Cr, BUN and ALB*

After 4 weeks of treatment, serum levels of Cr, BUN and ALB were observed as shown in Table 3. Compared to control group, serum levels of Cr and BUN were increased significantly in the UUO group ($p < 0.01$), UUO + SDG group ($p < 0.05$), UUO + Ad-P311 group ($p < 0.05$), and UUO + SDG + Ad-P311 ($p < 0.05$) group, while there was no significant difference between control group and control + Ad-P311 group ($p > 0.05$). Moreover, serum levels of Cr and BUN were reversed significantly by administration of SDG and Ad-P311 especially in UUO + SDG + Ad-P311 group ($p < 0.01$) compared to that in UUO group. Compared to control group, serum levels of

Table 2. The body weight of rats in different groups at beginning and end of experiments

Group	Body weight at the beginning of experiment (g)	Body weight at the end of experiment (g)
Control group	199.60 ± 8.64	402.00 ± 14.65
Control + Ad-P311 group	202.22 ± 8.11§	403.00 ± 13.18$^{\blacktriangle}$
UUO group	211.14 ± 11.25§	308.71 ± 15.22**
UUO + SDG group	201.88 ± 6.20§	356.38 ± 7.03$^{*\Delta}$
UUO + Ad-P311 group	201.12 ± 13.22§	365.25 ± 8.88$^{*\Delta}$
UUO + SDG + Ad-P311 group	205.33 ± 8.54§	379.00 ± 9.34$^{*\Delta\Delta}$

Note: Body weight at the beginning of experiment: $^{\S}p > 0.05$ *vs*. Control group; Body weight at the end of experiment: $^{\blacktriangle}p > 0.05$ *vs*. Control group, $^{*}p < 0.05$ *vs*. Control group, $^{**}p < 0.01$ *vs*. Control group, $^{\Delta}p < 0.05$ *vs*. UUO group, $^{\Delta\Delta}p < 0.01$ *vs*. UUO group.

Table 3. The serum levels of Cr, BUN and ALB of rats in different groups after 4 weeks of treatment

Group	Cr (μmol/L)	BUN (mmol/L)	ALB (g/L)
Control group	42.58 ± 2.95	6.33 ± 1.10	34.39 ± 1.66
Control + Ad-P311 group	41.22 ± 3.36$^{\Delta}$	7.03 ± 0.90$^{\Delta}$	33.31 ± 1.95$^{\Delta}$
UUO group	118.79 ± 6.14$^{\blacktriangle\blacktriangle}$	32.64 ± 4.02$^{\blacktriangle}$	22.57 ± 1.43$^{\blacktriangle\blacktriangle}$
UUO + SDG group	93.68 ± 6.36$^{\blacktriangle *}$	15.27 ± 1.28$^{\blacktriangle *}$	30.07 ± 1.11$^{\blacktriangle *}$
UUO + Ad-P311 group	76.23 ± 4.45$^{\blacktriangle *}$	12.37 ± 1.33$^{\blacktriangle *}$	25.13 ± 0.97$^{\blacktriangle *}$
UUO + SDG + Ad-P311 group	59.27 ± 4.94$^{\blacktriangle **}$	8.72 ± 1.20$^{\blacktriangle **}$	29.90 ± 1.08$^{\blacktriangle *}$

Note: $^{\Delta}p > 0.05$ *vs*. Control group, $^{\blacktriangle}p < 0.05$ *vs*. Control group, $^{\blacktriangle\blacktriangle}p < 0.01$ *vs*. Control group, $^{*}p < 0.05$ *vs*. UUO group, $^{**}p < 0.01$ *vs*.UUO group.

ALB were decreased significantly in UUO group ($p < 0.01$), UUO + SDG group ($p < 0.05$), UUO + Ad-P311 group ($p < 0.05$), and UUO + SDG + Ad-P311 ($p < 0.05$) group, while there was no significant difference between control group and control + Ad-P311 group ($p > 0.05$). Moreover, serum levels of ALB were reversed significantly by administration of SDG and Ad-P311 ($p < 0.05$) compared to that in UUO group.

3.3. *SDG combined with P311 attenuated UUO-induced fibrosis*

As shown in Figure 1A, HE staining demonstrated that there were no histological changes in kidneys of sham rats as shown in control group and control + Ad-P311 group, while kidneys developed remarkable pathological changes such as interstitial fibrosis, tubular expansion, atrophy and inflammatory cell invasion in UUO rats as shown in the UUO group. However, these histological lesions in the kidneys of UUO rats were attenuated by administration of SDG and Ad-P311 especially in UUO + SDG + Ad-P311 group compared to those in the UUO group. Consistent with pathological changes in experimental kidneys, UUO surgery resulted in about an 8-time increase of renal tubular injury index, but extent of damage was remarkably decreased from 83.20 ± 2.80% to 70.10 ± 3.82% by administration of SDG and Ad-P311 especially in the UUO + SDG + Ad-P311 group compared to that in UUO group ($p < 0.01$) (Figure 1B). As shown in Figure 2A, Masson staining showed that collagen deposition and fibrosis areas were significantly decreased by administration of SDG and Ad-P311 especially in the UUO + SDG + Ad-P311 group compared to those in the UUO group. Collagen accumulation had increased prominently about 3 fold in the interstitium of UUO kidneys, while administration

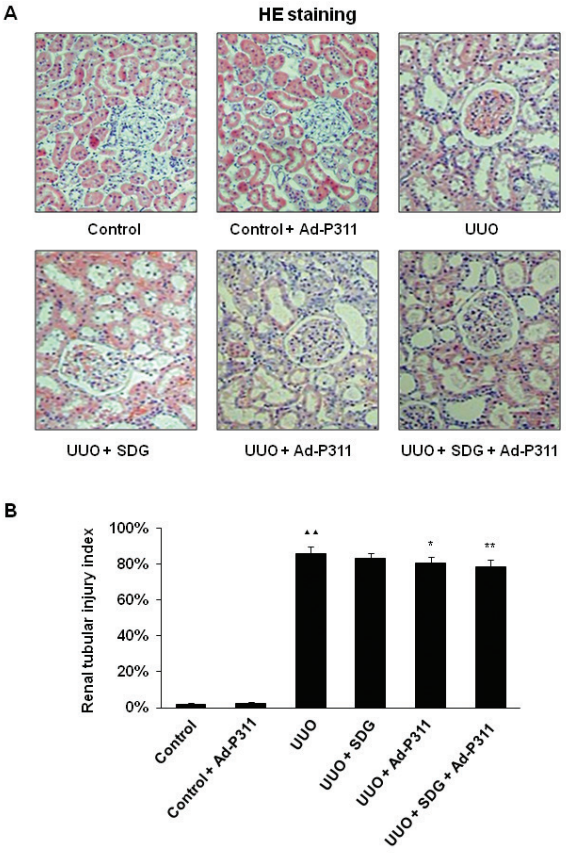

Figure 1. SDG combined with P311 attenuated UUO-induced pathological changes in the kidneys, which were detected by hematoxylin eosin (HE) staining. (A) HE staining (× 200); **(B)** The semi-quantitative accession of the renal tubular injury index in HE-stained sections of rat kidneys. $^{\blacktriangle\blacktriangle}p < 0.01$, compared to control group; $^{*}p < 0.05$, compared to UUO group; $^{**}p < 0.01$, compared to UUO group.

of SDG and Ad-P311 decreased the amount of collagen deposition from 2.94 ± 0.34 to 2.13 ± 0.30, compared to the UUO group ($p < 0.01$) (Figure 2B).

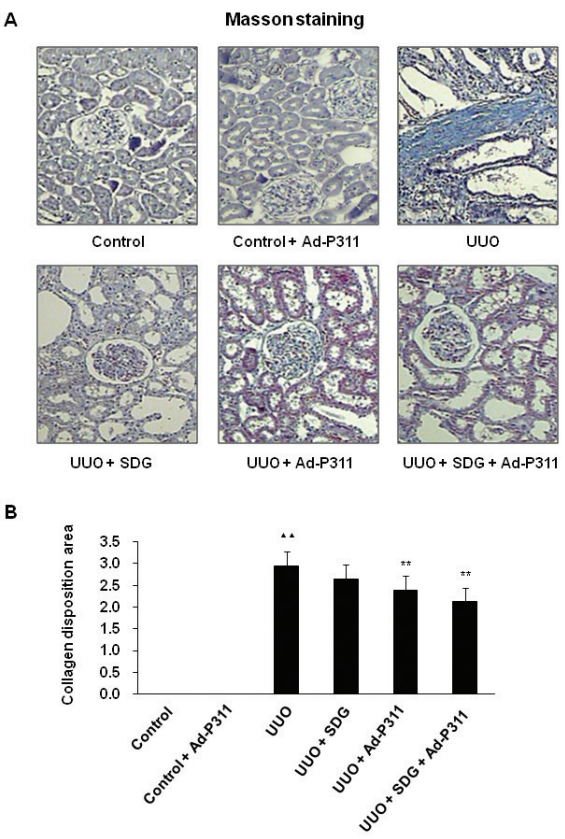

Figure 2. SDG combined with P311 attenuated UUO-induced pathological changes in the kidneys which were detected by Masson staining. (A) Masson staining (× 200); **(B)** The degree of interstitial collagen deposits in Masson-stained sections of rat kidneys. ▲▲$p < < 0.01$, compared to control group; **$p < 0.01$, compared to UUO group.

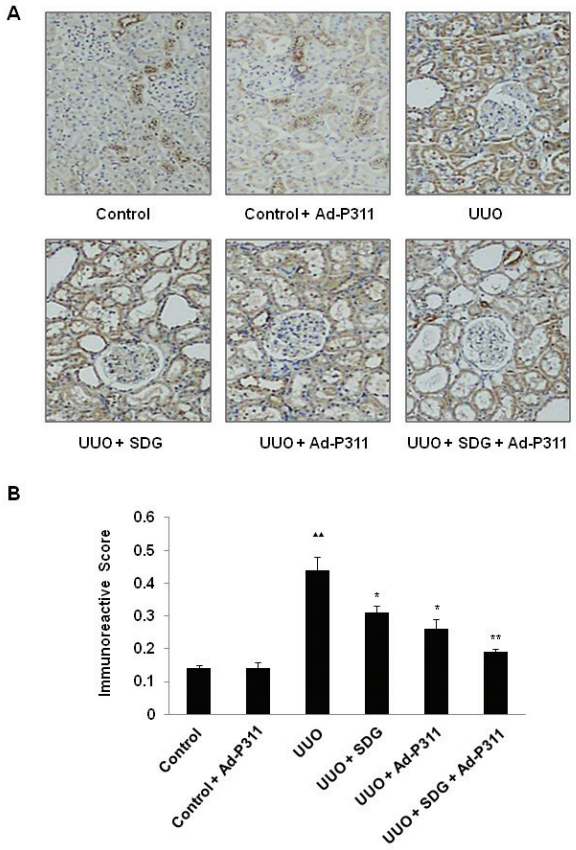

Figure 3. SDG combined with P311 reversed the expression α-SMA, which was detected by immunohistochemical staining in UUO kidneys. (A) Representative photomicrograph illustrating α-SMA expression in UUO kidneys; **(B)** Graph showing the immunoreactive score of α-SMA in UUO kidneys by quantitative morphometric analysis. ▲▲$p < 0.01$, compared to control group; *$p < 0.05$, compared to UUO group; **$p < 0.01$, compared to UUO group. Original magnifications, × 200.

3.4. *SDG combined with P311 reversed the expression α-SMA, pSmad2/3 and Smad7 detected by immunohistochemical staining in UUO Kidneys*

Protein expression of mesenchymal marker α-SMA was investigated by immunohistochemical staining to explore the effect of SDG and Ad-P311 on EMT related markers in UUO Kidneys. As shown in Figures 3A and 3B, protein expression of α-SMA was increased significantly in UUO kidneys compared to that in the sham operated control kidneys (control group and control + Ad-P311 group) ($p < 0.01$), while there was no significant difference between control group and control + Ad-P311 group ($p > 0.05$). In contrast, the increased expression of α-SMA in UUO kidneys was reversed by the administration of SDG and Ad-P311 especially in the UUO + SDG + Ad-P311 group ($p < 0.01$) compared to UUO group.

Protein expression of Smad2/3 and Smad7 was also investigated by immunohistochemical staining to explore the possible mechanism of SDG and Ad-P311 on EMT of UUO Kidneys. As shown in Figures 4A and 4B, the protein expression of pSmad2/3 was dramatically elevated in the UUO group compared with the sham groups (control group and control +Ad-P311 group) ($p < 0.01$), while there was no significant difference between control group and control + Ad-P311 group ($p > 0.05$). In contrast, SDG and Ad-P311 administration substantially ameliorated this elevation induced by UUO surgery. As shown in Figures 5A and 5B, protein expression of Smad7 was decreased significantly in UUO kidneys compared to that in the sham groups (control group and control + Ad-P311 group) ($p < 0.01$), while there was no significant difference between control group and control + Ad-P311 group ($p > 0.05$). In contrast, administration of SDG and Ad-P311 alleviated its decrease especially in UUO + SDG + Ad-P311 group ($p < 0.01$) compared to UUO group.

3.5. *SDG combined with P311 reversed the expression of EMT related proteins detected by Western blot analysis in UUO Kidneys*

To further explore the effect of SDG and Ad-P311 on EMT related markers in UUO Kidneys, expression of epithelial marker E-cadherin and mesenchymal marker

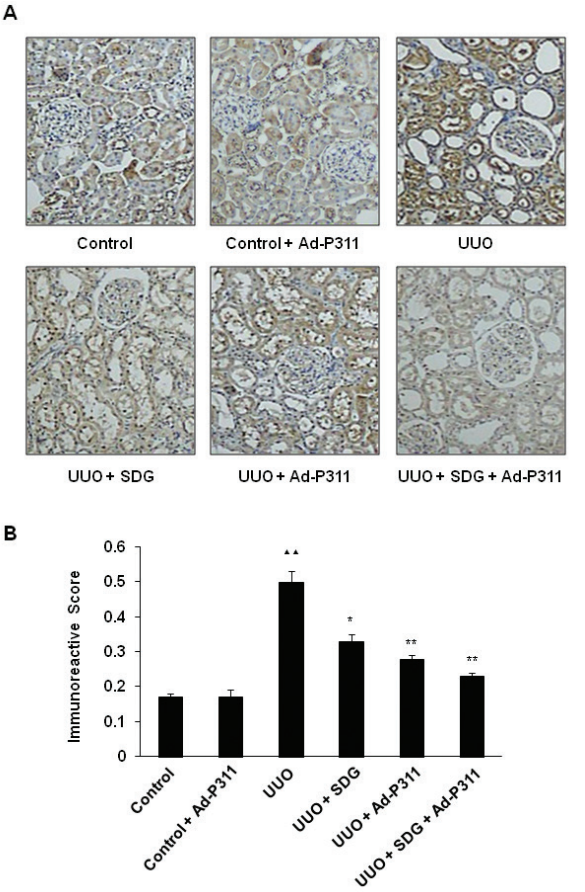

Figure 4. SDG combined with P311 reversed the expression pSmad2/3, which was detected by immunohistochemical staining in UUO kidneys. (A) Representative photomicrograph illustrating pSmad2/3 expression in UUO kidneys; **(B)** Graph showing the immunoreactive score of pSmad2/3 in UUO kidneys by quantitative morphometric analysis. ▲▲$p < 0.01$, compared to control group; *$p < 0.05$, compared to UUO group; **$p < 0.01$, compared to UUO group. Original magnifications, × 200.

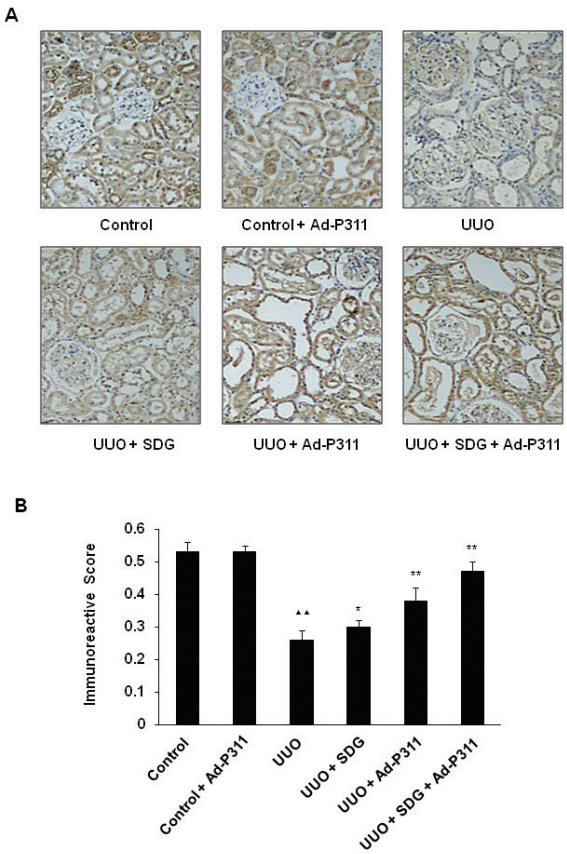

Figure 5. SDG combined with P311 reversed the expression of Smad7, which was detected by immunohistochemical staining in UUO kidneys. (A) Representative photomicrograph illustrating Smad7 expression in UUO kidneys; **(B)** Graph showing the immunoreactive score of Smad7 in UUO kidneys by quantitative morphometric analysis. ▲▲$p < 0.01$, compared to control group; *$p < 0.05$, compared to UUO group; **$p < 0.01$, compared to UUO group. Original magnifications, × 200.

α-SMA in UUO kidneys was examined by Western blot analysis. As shown in Figures 6A and 6B, the protein level of E-cadherin was decreased significantly in the UUO group compared with sham groups (control group and control +Ad-P311 group) ($p < 0.01$), while there was no significant difference between control group and control + Ad-P311 group ($p > 0.05$). However, administration of SDG and Ad-P311 alleviated its decrease. The protein expression of α-SMA was increased significantly in UUO kidneys compared to that in the sham operated control kidneys ($p < 0.01$), while there was no significant difference between control group and control + Ad-P311 group ($p > 0.05$). However, the increased expression of α-SMA in UUO kidneys was reversed by administration of SDG and Ad-P311 (Figures 6A and 6B).

To explore possible mechanism of SDG and Ad-P311 on EMT of UUO Kidneys, the protein expression of EMT related molecules TGF-β1, pSmad2/3, Smad7, and ILK were measured by Western blot analysis. As shown in Figures 7A and 7B, protein expression of TGF-β1, pSmad2/3, and ILK was increased significantly in UUO kidneys compared to that in the sham operated control kidneys (control group and control +Ad-P311 group) ($p < 0.01$), while there was no significant difference between control group and control + Ad-P311 group ($p > 0.05$). However, administration of SDG and Ad-P311 alleviated all of the above changes significantly. Protein expression of Smad7 was decreased significantly in UUO kidneys compared to that in the sham operated control kidneys (control group and control +Ad-P311 group) ($p < 0.01$), while there was no significant difference between control group and control + Ad-P311 group (p > 0.05). However, the decreased expression of Smad7 in UUO kidneys was reversed by administration of SDG and Ad-P311 (Figures 7A and 7B).

4. Discussion

As a traditional Chinese herbal formula, SDG has been used clinically for treatment of CKD for many years (*4*). Radix Astragali and Salvia miltiorrhiza are the two

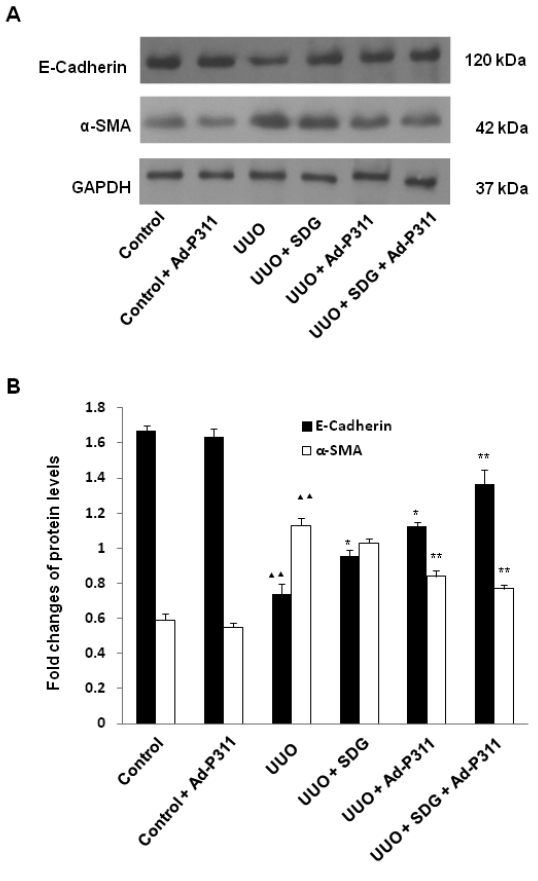

Figure 6. SDG combined with P311 reversed the expression of EMT markers (E-cadherin and α-SMA), which was detected by Western blot analysis in UUO Kidneys. (A) Expression of E-cadherin and α-SMA at the protein level in each group was determined with GAPDH used as an internal control. **(B)** The expression level of E-cadherin and α-SMA was quantitatively analyzed with Image J software. ▲▲$p <$ 0.01, compared to control group; *$p < 0.05$, compared to UUO group; **$p < 0.01$, compared to UUO group.

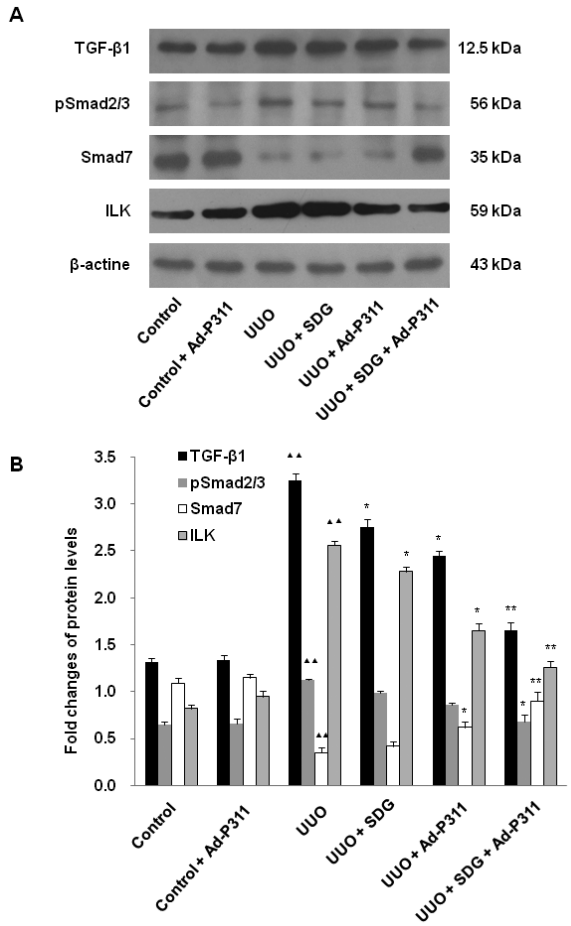

Figure 7. SDG combined with P311 reversed the expression of EMT related proteins TGF-β1, pSmad2/3, Smad7, and ILK, which was detected by Western blot analysis in UUO Kidneys. (A) Expression of TGF-β1, pSmad2/3, Smad7, and ILK at the protein level in each group was determined with β-actin used as an internal control. **(B)** The expression level of TGF-β1, pSmad2/3, Smad7, and ILK was quantitatively analyzed with Image J software. ▲▲$p < 0.01$, compared to control group; *$p < 0.05$, compared to UUO group; **$p < 0.01$, compared to UUO group.

principal ingredients of SDG, which play important roles in CKD treatment. A systematic review has shown that Radix Astragali used alone as a crude herb could offer some promising effects in reducing proteinuria and increasing hemoglobin and ALB in patients with CKD (*29*). Pharmacological studies have suggested that some formulas with Radix Astragali as a principal ingredient and some active compounds from Radix Astragali (*e.g.*, Astragaloside IV) are capable of ameliorating renal fibrosis *via* the TGF-β/Smad signaling pathway (*30,31*). In addition, Salvia miltiorrhiza and its active ingredients (*e.g.*, Tanshinone IIA) have proved to possess a protective effect on kidney injury by suppressing production of reactive oxygen species (ROS) (*32*) and regulating levels of TGF-β1 and collagen IV (*33*). Therefore, the inhibitory effect of Radix Astragali and Salvia miltiorrhiza on renal fibrosis might be one of the important mechanisms of SDG as an effective treatment for CKD.

Our previous studies indicated that SDG could effectively reduce kidney damage and prevent progression of CKD with a possible mechanism involved in the TGF-β1-Smad pathway (*5-7*). We also found P311 might be involved in the pathogenesis of renal fibrosis by inhibiting the EMT process *via* the TGF-β1-Smad-ILK pathway *in vitro* (*23*). Moreover, SDG combined with P311 could ameliorate renal fibrosis and block progression of CKD by regulating expression of the EMT-related protein α-SMA (*24*). Here we further examined the effect and mechanism of SDG combined with P311 on TGF-β1-mediated EMT in a rat model of UUO renal fibrosis. We found that SDG combined with P311 could protect kidney function of UUO rats *via* improving Cr, BUN, and ALB serum levels. We also found that SDG combined with P311 could attenuate histological lesions including interstitial fibrosis, tubular expansion, and atrophy and inflammatory cell invasion in kidneys of UUO rats, and the underlying mechanism might involve EMT and the TGF-β1-Smad-ILK signaling pathway.

Renal fibrosis is an inevitable outcome of all kinds of progressive CKD. It is characterized by the trans-differentiation of myofibroblasts and excessive accumulation of ECM (*8*). Chronic inflammation is considered a major contributor to nephropathic changes, including renal fibrosis (*15*). During the process of renal fibrosis, inflammatory cells infiltrate and produce several molecules, such as growth factors, angiogenic factors, profibrotic cytokines, and proteinases. All of these factors can stimulate excessive accumulation of ECM through EMT, which results in renal fibrosis. Among these, profibrotic cytokine TGF-β1 is proposed to be a major regulator in inducing EMT and the generation of interstitial fibroblasts (*12,13*). It can induce the activation of fibroblasts to undergo a phenotypic transition to myofibroblasts with tubular epithelial cells losing their adhesion molecules (such as E-cadherin), and gaining mesenchymal cell markers (such as α-SMA) (*11*). In the current study, expression of TGF-β1 was increased significantly in UUO kidneys, but administration of SDG and Ad-P311 alleviated its increase. Moreover, α-SMA expression was increased significantly and E-cadherin expression was decreased significantly in UUO kidneys, while the changed expression of α-SMA and E-cadherin in UUO kidneys was reversed by the administration of SDG and Ad-P311. Therefore, consistent with previous reports, TGF-β1 is the most potent inducer capable of initiating and completing the entire EMT course. SDG combined with P311 could prevent TGF-β1-mediated EMT in UUO kidneys.

The TGF-β1/Smad signaling pathway plays a key role in initiating and completing the entire EMT course in fibrotic disease pathogenesis (*34*). Currently, eight different Smad proteins have been found in vertebrates. Smad protein, because it is the most important downstream signal transduction molecule of TGF-β1 in cells, transfers the TGF-β1 signal from cell surface to nucleus, which can regulate target gene transcription. After TGF-β1 binds to its receptor Tβ R II and recruits Tβ R I, the activated complex directly phosphorylates downstream receptor-regulated Smads (R-Smads, including Smad1, 2, 3, 5, and 8). Phosphorylated R-Smads (*e.g.*, Smad2/3), binds to the common partner Smad4 and forms the Smad complex that translocates into the nucleus to initiate gene transcription and regulate cell behavior. Another class of Smads is inhibitory Smads (I-Smads, including Smad6 and Smad7), which can competitively combine with TGF-β1 receptor, preventing phosphorylation of R-Smads (*35*). In renal fibrosis, Smad2/3 is reported as a key EMT regulatory molecule inducing EMT and collagen accumulation, while Smad7 is reported to have a renoprotective effect through blocking the profibrotic effect of TGF-β and inhibiting Smad2/3 activation (*11,36*). Here we found that pSmad2/3 expression was increased and Smad7 expression was decreased significantly in UUO kidneys, but administration of SDG and Ad-P311 alleviated all of the above changes significantly. These results indicated that SDG combined with P311 not only regulates TGF-β1 but also the Smad signaling pathway. ILK is an intracellular serine/threonine protein kinase that interacts with the cytoplasmic domains of β-integrins and mediates integrin signaling in diverse types of cells (*11*). TGF-β1 mediated EMT has been suggested to be dependent on ILK function in a Smad-dependent manner during renal fibrosis (*15*). Here we found that ILK expression was increased significantly in UUO kidneys, however, administration of SDG and Ad-P311 significantly reversed the above changes. Taken together, these findings indicated that SDG combined with P311 attenuated TGF-β1-mediated EMT by regulating protein expression of pSmad2/3, Smad7 and ILK in UUO kidneys.

P311 is an intracytoplasmic protein that can bind to TGF-β latent associated protein and down-regulate expression of TGF-β1 and TGF-β2 (*17*). It has been shown to be of importance in the process of myofibroblast differentiation and fibrosis with functions of promoting embryonic development, wound healing, as well as nerve and lung regeneration, and so on (*18,20-22*). Pan *et al*. reported that P311 could block TGF-β1 signaling and cause an inhibition in collagen expression in myofibroblast transformation, suggesting that P311 might be involved in preventing fibrosis during wound repair (*18*). In our previous study, P311 could ameliorate renal fibrosis by blocking TGF-β1-mediated EMT *via* the TGF-β1-Smad-ILK pathway *in vitro* and UUO rats (*24*). However, Yao *et al*. found that P311 could promote renal fibrosis *via* TGFβ1/Smad signaling in the UUO model (*36*). This finding differs from our data. The relationship between P311 and TGF-β1 might be reasonable to explain this discrepancy, because infiltration of inflammatory cells is an early and characteristic feature of renal fibrosis (*37*). During renal fibrosis, at early stages of repair with abundant inflammatory cells, the antifibrogenic effect of P311 may be offset by TGF-β1 and exhibit a pro-fibrogenic effect, while at advanced stages of repair while inflammatory cells gradually disappeared, the antifibrogenic effect of P311 may increase over time and become maximal toward the end of the reparative process (*18*). Thus, here we found that SDG combined with P311 could ameliorate renal fibrosis by blocking the TGF-β1/Smad signaling pathway in UUO rats. Although SDG has the potential to be a cost-effective and safe treatment for renal fibrosis, further studies are needed to verify the active components of this herbal medicine.

5. Conclusions

In summary, our data present that SDG combined with P311 could attenuate renal fibrosis in UUO rats, and the underlying mechanism might involve TGF-β1-mediated EMT and the TGF-β1-Smad-ILK signaling pathway.

Therefore, SDG might be a novel alternative therapy for treatment of renal fibrosis and progression of CKD. Furthermore, SDG combined with P311 might have a synergistic effect on attenuating renal fibrosis. Taken together, these findings provide a new way for treatment of CKD.

Acknowledgements

The current work was supported by the National Natural Science Foundation of China (No. 81273682) and the Science and Technology Development Program of Shandong Province (No. 2010G0020220).

References

1. Romagnani P, Remuzzi G, Glassock R, Levin A, Jager KJ, Tonelli M, Massy Z, Wanner C, Anders HJ. Chronic kidney disease. Nat Rev Dis Primers. 2017; 3:17088.
2. Liu Y. Cellular and molecular mechanisms of renal fibrosis. Nat Rev Nephrol. 2011; 7:684-696.
3. Zhong Y, Deng Y, Chen Y, Chuang PY, Cijiang He J. Therapeutic use of traditional Chinese herbal medications for chronic kidney diseases. Kidney Int. 2013; 84:1108-1118.
4. Peng M, Cai P, Ma H, Meng H, Xu Y, Zhang X, Si G. Chinese herbal medicine Shenqi Detoxification Granule inhibits fibrosis in adenine induced chronic renal failure rats. Afr J Tradit Complement Altern Med. 2013;11:194-204.
5. Li Y, Si GM, Zhang Y, Hu YS. Effect of the Shenqi Jiedu decoction on chronic renal failure: an experimental study. Journal of Shandong University (Health Science). 2007; 45:1015-1018. (in Chinese)
6. Zhang Y, Si GM, Xu DM, Li Y. Clinical observation of "Shenqi Jiedu Decoction" in treating chronic renal failure of turbidity and blood-stasis syndrome and its effects on peripheral blood adhesion molecule. Shanghai Journal of Traditional Chinese Medicine. 2008; 42:26-28. (in Chinese)
7. Li TT, Si GM, Chen FC. Effects of Shenqi Jiedu Decoction on expression of transforming growth factor-β1, smad2 and smad3 in renal tissues of rats with chronic renal failure induced by adenine. Zhong Xi Yi Jie He Xue Bao. 2010; 8:263-268. (in Chinese)
8. Qi W, Chen X, Poronnik P, Pollock CA. The renal cortical fibroblast in renal tubulointerstitial fibrosis. Int J Biochem Cell Biol. 2006; 38:1-5.
9. Kanasaki K, Taduri G, Koya D. Diabetic nephropathy: the role of inflammation in fibroblast activation and kidney fibrosis. Front Endocrinol (Lausanne). 2013; 4:7.
10. Iwano M, Plieth D, Danoff TM, Xue C, Okada H, Neilson EG. Evidence that fibroblasts derive from epithelium during tissue fibrosis. J Clin Invest. 2002; 110:341-350.
11. Liu Y. New insights into epithelial-mesenchymal transition in kidney fibrosis. J Am Soc Nephrol. 2010; 21:212-222.
12. Pohlers D, Brenmoehl J, Löffler I, Müller CK, Leipner C, Schultze-Mosgau S, Stallmach A, Kinne RW, Wolf G. TGF-beta and fibrosis in different organs - molecular pathway imprints. Biochim Biophys Acta. 2009; 1792:746-756.
13. Wang Q, Wang Y, Huang X, Liang W, Xiong Z, Xiong Z. Integrin β4 in EMT: an implication of renal diseases. Int J Clin Exp Med. 2015; 8:6967-6976.
14. Jia L, Ma X, Gui B, Ge H, Wang L, Ou Y, Tian L, Chen Z, Duan Z, Han J, Fu R. Sorafenib ameliorates renal fibrosis through inhibition of TGF-β-induced epithelial-mesenchymal transition. PLoS One. 2015; 10:e0117757.
15. Kim MK, Maeng YI, Sung WJ, Oh HK, Park JB, Yoon GS, Cho CH, Park KK. The differential expression of TGF-β1, ILK and wnt signaling inducing epithelial to mesenchymal transition in human renal fibrogenesis: an immunohistochemical study. Int J Clin Exp Pathol. 2013; 6:1747-1758.
16. Li Y, Yang J, Dai C, Wu C, Liu Y. Role for integrin-linked kinase in mediating tubular epithelial to mesenchymal transition and renal interstitial fibrogenesis. J Clin Invest. 2003; 112:503-516.
17. Paliwal S, Shi J, Dhru U, Zhou Y, Schuger L. P311 binds to the latency associated protein and downregulates the expression of TGF-beta1 and TGF-beta2. Biochem Biophys Res Commun. 2004; 315:1104-1109.
18. Pan D, Zhe X, Jakkaraju S, Taylor GA, Schuger L. P311 induces a TGF-beta1-independent, nonfibrogenic myofibroblast phenotype. J Clin Invest. 2002; 110:1349-1358.
19. Mariani L, McDonough WS, Hoelzinger DB, Beaudry C, Kaczmarek E, Coons SW, Giese A, Moghaddam M, Seiler RW, Berens ME. Identification and validation of P311 as a glioblastoma invasion gene using laser capture microdissection. Cancer Res. 2001; 61:4190-4196.
20. Fujitani M, Yamagishi S, Che YH, Hata K, Kubo T, Ino H, Tohyama M, Yamashita T. P311 accelerates nerve regeneration of the axotomized facial nerve. J Neurochem. 2004; 91:737-744.
21. Zhao L, Leung JK, Yamamoto H, Goswami S, Kheradmand F, Vu TH. Identification of P311 as a potential gene regulating alveolar generation. Am J Respir Cell Mol Biol. 2006; 35:48-54.
22. Tan J, Peng X, Luo G, Ma B, Cao C, He W, Yuan S, Li S, Wilkins JA, Wu J. Investigating the role of P311 in the hypertrophic scar. PLoS One. 2010; 5:e9995.
23. Qi FH, Cai PP, Liu X, Peng M, Si GM. Adenovirus-mediated P311 inhibits TGF-β1-induced epithelialmesenchymal transition in NRK-52E cells *via* TGF-β1-Smad-ILK pathway. BioSci Trends. 2015; 9:299-306.
24. Gao R, Liu R, Si GM. Effect on the expression of α-SMA and α-SMA mRNA with Shenqi Jiedu Decoction combined with P311 in the Process of renal interstitial fibrosis. World Journal of Integrated Traditional and Western Medicine. 2016; 11:41-43. (in Chinese)
25. Baba I, Egi Y, Utsumi H, Kakimoto T, Suzuki K. Inhibitory effects of fasudil on renal interstitial fibrosis induced by unilateral ureteral obstruction. Mol Med Rep. 2015; 12:8010-8020.
26. Yin Y, Qi F, Song Z, Zhang B, Teng J. Ferulic acid combined with astragaloside IV protects against vascular endothelial dysfunction in diabetic rats. Biosci Trends. 2014; 8:217-226.
27. Liu QF, Ye JM, Deng ZY, Yu LX, Sun Q, Li SS. Ameliorating effect of Klotho on endoplasmic reticulum stress and renal fibrosis induced by unilateral ureteral obstruction. Iran J Kidney Dis. 2015; 9:291-297.
28. Lu H, Dong J, Zhang Y, Li C, Yu Q, Tang W. Pathological changes in primary cilia: a novel mechanism of graft cholangiopathy caused by prolonged cold preservation

in a rat model of orthotopic liver transplantation. Biosci Trends. 2014; 8:206-211.
29. Zhang HW, Lin ZX, Xu C, Leung C, Chan LS. Astragalus (a traditional Chinese medicine) for treating chronic kidney disease. Cochrane Database Syst Rev. 2014; 10:CD008369.
30. Zhao J, Wang L, Cao AL, Jiang MQ, Chen X, Wang Y, Wang YM, Wang H, Zhang XM, Peng W. HuangQi decoction ameliorates renal fibrosis *via* TGF-β/Smad signaling pathway *in vivo* and *in vitro*. Cell Physiol Biochem. 2016; 38:1761-1774.
31. Wang L, Chi YF, Yuan ZT, Zhou WC, Yin PH, Zhang XM, Peng W, Cai H. Astragaloside IV inhibits renal tubulointerstitial fibrosis by blocking TGF-β/Smad signaling pathway *in vivo* and *in vitro*. Exp Biol Med (Maywood). 2014; 239:1310-1324.
32. Lu X, Jin Y, Ma L, Du L. Danshen (Radix Salviae Miltiorrhizae) reverses renal injury induced by myocardial infarction. J Tradit Chin Med. 2015; 35:306-311.
33. Ahn YM, Kim SK, Lee SH, Ahn SY, Kang SW, Chung JH, Kim SD, Lee BC. Renoprotective effect of Tanshinone IIA, an active component of Salvia miltiorrhiza, on rats with chronic kidney disease. Phytother Res. 2010; 24:1886-1892.
34. O'Connor JW, Gomez EW. Biomechanics of TGFβ-induced epithelial-mesenchymal transition: implications for fibrosis and cancer. Clin Transl Med. 2014; 3:23.
35. Wang W, Koka V, Lan HY. Transforming growth factor-beta and Smad signalling in kidney diseases. Nephrology (Carlton). 2005; 10:48-56.
36. Yao Z, Yang S, He W, Li L, Xu R, Zhang X, Li H, Zhan R, Sun W, Tan J, Zhou J, Luo G, Wu J. P311 promotes renal fibrosis *via* TGFβ1/Smad signaling. Sci Rep. 2015; 5:17032.
37. Chen G, Chen H, Wang C, Peng Y, Sun L, Liu H, Liu F. Rapamycin ameliorates kidney fibrosis by inhibiting the activation of mTOR signaling in interstitial macrophages and myofibroblasts. PLoS One. 2012; 7:e33626.

(Received November 7, 2017; Revised December 14, 2017; Accepted December 25, 2017)